

The British University in Egypt

BUE Scholar

Pharmacy

Health Sciences

1-10-2023

Exploring the potential of intranasally administered naturally occurring quercetin loaded into polymeric nanocapsules as a novel platform for the treatment of anxiety

Shady Swidan

The British University in Egypt, shady.swidan@bue.edu.eg

Khaled Younis Mahmoud


Nahla Ahmed Elhesaisy

Abdelrahman Rashed

Ebram Mikhael

See next page for additional authors

Follow this and additional works at: <https://buescholar.bue.edu.eg/pharmacy>

 Part of the [Animal Experimentation and Research Commons](#), [Other Pharmacology, Toxicology and Environmental Health Commons](#), and the [Other Pharmacy and Pharmaceutical Sciences Commons](#)

Recommended Citation

Swidan, Shady; Mahmoud, Khaled Younis; Elhesaisy, Nahla Ahmed; Rashed, Abdelrahman; Mikhael, Ebram; Fadl, Mahmoud; Elsadek, Mahmoud; Mohamed, Merna; Mostafa, Merna; Hassan, Mohamed; Halema, Omar; and Elnemer, Youssef, "Exploring the potential of intranasally administered naturally occurring quercetin loaded into polymeric nanocapsules as a novel platform for the treatment of anxiety" (2023). *Pharmacy*. 603.

<https://buescholar.bue.edu.eg/pharmacy/603>

This Article is brought to you for free and open access by the Health Sciences at BUE Scholar. It has been accepted for inclusion in Pharmacy by an authorized administrator of BUE Scholar. For more information, please contact bue.scholar@gmail.com.

Authors

Shady Swidan, Khaled Younis Mahmoud, Nahla Ahmed Elhesaisy, Abdelrahman Rashed, Ebram Mikhael, Mahmoud Fadl, Mahmoud Elsadek, Merna Mohamed, Merna Mostafa, Mohamed Hassan, Omar Halema, and Youssef Elnemer



OPEN

Exploring the potential of intranasally administered naturally occurring quercetin loaded into polymeric nanocapsules as a novel platform for the treatment of anxiety

Khaled Y. Mahmoud^{1,3}, Nahla A. Elhesaisy^{1,3}, Abdelrahman R. Rashed², Ebram S. Mikhael², Mahmoud I. Fadl², Mahmoud S. Elsadek², Merna A. Mohamed², Merna A. Mostafa², Mohamed A. Hassan², Omar M. Halema², Youssef H. Elnemer² & Shady A. Swidan¹✉

Anxiety is one of the most prevalent forms of psychopathology that affects millions worldwide. It gained more importance under the pandemic status that resulted in higher anxiety prevalence. Anxiolytic drugs such as benzodiazepines have an unfavorable risk/benefit ratio resulting in a shift toward active ingredients with better safety profile such as the naturally occurring quercetin (QRC). The delivery of QRC is hampered by its low water solubility and low bioavailability. The potential to enhance QRC delivery to the brain utilizing polymeric nanocapsules administered intranasally is investigated in the current study. Polymeric nanocapsules were prepared utilizing the nanoprecipitation technique. The best formula displayed a particle size of 227.8 ± 11.9 nm, polydispersity index of 0.466 ± 0.023 , zeta potential of -17.5 ± 0.01 mV, and encapsulation efficiency % of $92.5 \pm 1.9\%$. In vitro release of QRC loaded polymeric nanocapsules exhibited a biphasic release with an initial burst release followed by a sustained release pattern. Behavioral testing demonstrated the superiority of QRC loaded polymeric nanocapsules administered intranasally compared to QRC dispersion administered both orally and intranasally. The prepared QRC loaded polymeric nanocapsules also demonstrated good safety profile with high tolerability.

Abbreviations

APA	American Psychological Association
BBB	Blood–brain barrier
DSC	Differential scanning calorimetry
EE	Encapsulation efficiency
GABA	γ -Aminobutyric acid
GBD	Global burden of diseases, injuries, and risk factors study
H&E	Hematoxylin and eosin
HSP	Hansen solubility parameters
HSPiP	Hansen solubility parameters in practice
PCL	Polycaprolactone
PDI	Polydispersity Index
QRC	Quercetin
SD	Standard deviation

¹Department of Pharmaceutics and Pharmaceutical Technology, Faculty of Pharmacy, The British University in Egypt, El-Sherouk City 11837, Cairo, Egypt. ²Faculty of Pharmacy, The British University in Egypt, El-Sherouk City 11837, Cairo, Egypt. ³These authors contributed equally: Khaled Y. Mahmoud and Nahla A. Elhesaisy. ✉email: shady.swidan@bue.edu.eg

SEM	Standard error of mean
TEM	Transmission electron microscopy
XRD	X-Ray diffraction

Anxiety is defined by the American Psychological Association (APA) as “an emotion characterized by feelings of tension, worried thoughts and physical changes like increased blood pressure”¹. The Global Burden of Diseases, Injuries, and Risk Factors Study (GBD) 2019 identified anxiety disorders as the most prominent mental disorder. This high prevalence was present for both sexes, and across the entire lifespan². World struck Covid-19 pandemic resulted in intensifying the already high prevalence of anxiety. Daily infection rates and human mobility reductions were associated with increased anxiety prevalence³.

Anxiety disorders are characterized by enduring and excessive fear, and avoidance of perceived threats such as social situations or body sensations. Also, panic attacks can manifest as a form of abrupt fear response⁴. Anxiety disorders can be classified into specific phobia, generalized anxiety disorder, social anxiety disorder, agoraphobia, and panic disorder⁵. Multiple treatment options for anxiety disorders including azapirones, benzodiazepines, serotonin norepinephrine reuptake inhibitors, antipsychotics, antihistamines, and alpha- and beta-adrenergic medications⁶.

Despite the presence of multiple classes of anxiety treatment, full disease treatment is still un-achievable. Conventional pharmacological approaches are characterized by multiple side effects and poor tolerability profile⁷. The need for active ingredients with higher safety profile promoted a shift toward phytochemicals. Phytochemicals are low molecular weight secondary metabolites that exist naturally in plants⁸. Among the different phytochemicals present, Quercetin (QRC) was reported as an anxiolytic⁹.

QRC (2-(3,4-dihydroxyphenyl)-3,5,7-trihydroxychromen-4-one) is one of the most common flavonoids of polyphenols present in many plants such as red onions and kale¹⁰. QRC has a large spectrum of reported pharmacological actions ranging from anti-diabetic effects to anti-cancer effects¹¹ aside from its reported anxiolytic effect. Multiple articles reported the effects of QRC on anxiety. These articles are summarized in a previously published review article by Silvestro et al.¹².

Different mechanisms have been reported previously for the anxiolytic effects of QRC. One of these mechanisms is the chelation of iron overload in the brain. It has been reported that 3-hydroxyl and 4-carbonyl groups of QRC are the potential iron chelating sites^{13–15}. Other reported mechanisms include the modulation of corticosterone, γ -aminobutyric acid (GABA), and serotonin^{16,17}.

Despite the huge benefits of QRC, its use is hampered by its low water solubility and low oral bioavailability¹⁸. One of the most common approaches to overcome these limitations is the utilization of nanoparticles. Nanoparticles are defined as 3D objects with 3 external dimensions in the nano range with the nano range ranging from 1 and 1000 nm¹⁹.

QRC have been previously incorporated in different lipid based nanoparticles for the treatment of anxiety and anxiety related disorders^{17,20–22}. Despite the advantages of the prepared formulations, lipid based nanoparticles possess some limitations that may hamper their effective usage including short half-life, risk of oxidation and hydrolysis of the used phospholipid and risk of drug expulsion²³.

Among the different classes of nanoparticles, polymeric nanoparticles have generated great interest because of their advantages. These advantages including controlled drug release, biocompatibility, biodegradability, and drug protection against the environment²⁴. Polymeric nanoparticles can be classified into nanospheres and nanocapsules. Nanospheres compose of homogenous solid polymeric matrix while nanocapsules consist of liquid/solid core surrounded by a polymeric shell. Over recent years, polymeric nanocapsules attracted significant interest in the drug delivery field. This interest can be attributed to the higher drug loading capacity and lower polymer content compared to polymeric nanospheres²⁵.

Among the various available routes of administration, intranasal route is the preferred route of administering active pharmaceutical ingredients directly to the brain²⁶. The intranasal pathway allows for either delivery of therapeutics directly to the brain from the nose bypassing the blood–brain barrier (BBB) by traveling extracellularly along the olfactory and trigeminal nerve pathways, or through the vasculature route followed by system circulation in which passing the BBB is required²⁷. Nanoparticles possess multiple advantages rendering them ideal candidates for intranasal delivery such as thermodynamic stability, and the ability to penetrate biological membranes including the BBB^{28,29}.

Despite the high prevalence of anxiety, concurrently higher disease burden, there have been far lower number of recent research on novel anxiety treatments compared to number of experimental drugs for other disorders such as major depressive disorder, and schizophrenia⁶. The aim of the present study is to prepare and evaluate for the first time -to the best of our knowledge- QRC loaded polymeric nanocapsules as an anxiety treatment utilizing the intranasal route. The effect of amount of drug and the type of surfactant on the polymeric nanocapsules characteristics was evaluated and in vivo behavioral assessments were conducted.

Materials and methods

Materials. QRC ($\geq 95\%$), Polycaprolactone (PCL)-Mwt. 14000, and Benzalkonium Chloride were purchased from Sigma-Aldrich (St. Louis, MO, USA). Tween 80, and Poloxamer 188 (Pluronic F68) were purchased from Alfa Aesar (Lancashire, United Kingdom). Span 80 (Sorbitan Mono-oleate) was purchased from Oxford Laboratory Chemicals (Maharashtra, India). Capryol 90 (Propylene glycol monocaprylate) was a kind gift from Gattefosse (Saint-Priest, Cedex, France). Acetone analytical grade was purchased from Piochem (Giza, Egypt). All chemicals were used as received without modifications.

Theoretical screening of QRC solubility in different liquid lipids. Hansen Solubility Parameters (HSP) were used to theoretically predict the miscibility between QRC and twelve different liquid lipids namely Capryol 90, Capryol PGMC, Captex 200P, Captex 355, Ethyl Oleate, Isopropyl Myristate, Labrafil M 1944 CS, Labrafil M 2125 CS, Labrafac Lipophile WL 1349, Labrafac PG, Miglyol 810, and Oleic Acid. HSP of QRC and different liquid lipids were calculated using version 5.3.06 Hansen Solubility Parameters in Practice (HSPiP) software (Hansen Solubility, Hørsholm, Denmark) employing Hiroshi Yamamoto's molecular breaking method (Y-MB). The chemical structures of different materials were obtained using ChemBioDraw Ultra version 14.0 (CambridgeSoft corporation, Cambridge, MA, USA) through utilizing the IUPAC name of each material from PubChem database (available from <https://pubchem.ncbi.nlm.nih.gov/>). Each structure was converted by ChemBioDraw Ultra software to its simplified molecular input line entry syntax (SMILES) notation to be fed to HSPiP software generating the different solubility parameters in silico. The solubility parameters obtained were δ_D , which refers to dispersion forces (van der Waals), δ_P that refers dipole forces (polarity), and δ_H which refers to hydrogen bonding. Euclidean distance [Eq. (1)] was used to predict the solubility between QRC and different lipids where solute refers to QRC and solvent refers to the lipids³⁰.

$$D = \sqrt{(\delta D(\text{solute}) - \delta D(\text{solvent}))^2 + (\delta P(\text{solute}) - \delta P(\text{solvent}))^2 + (\delta H(\text{solute}) - \delta H(\text{solvent}))^2} \quad (1)$$

Solubility study. QRC solubility in Capryol 90 was determined using a modified shake method³¹. Excess amount of QRC was added to one gram of Capryol 90 in a glass vial. The prepared dispersion was placed in a shaking water bath (Sci Finetech Shaking Water Bath, Korea) set at 25 ± 0.5 °C and 50 RPM for 24 h. The undissolved QRC was removed through centrifugation for 1 h at 12,000 RPM and 25 °C (PRO-Research K241R; Centurion, West Sussex, United Kingdom). The obtained supernatant was appropriately diluted and measured spectrophotometrically at $\lambda_{\text{max}} = 367$ nm using UV spectrophotometer (Jenway 6305 spectrophotometer, China).

Preparation of QRC loaded polymeric nanocapsules. Polymeric nanocapsules entrapping QRC were prepared using a modified nanoprecipitation method³². QRC, PCL (100 mg), span 80 (40 mg), and Capryol 90 (90 μ l) were dissolved together in 25 ml acetone to prepare the organic phase. The aqueous phase was prepared by dissolving the surfactant in 50 ml distilled water. The prepared organic phase was added drop wise onto the aqueous phase under moderate stirring to allow for the formation of nanocapsules. The prepared nano-dispersion was added into a round bottom flask placed in a rotary evaporator (SCIOLOGEX Rotary Evaporator Rotavapor RE100-Pro; SCIOLOGEX, Rocky Hill, CT, USA) set at 40 °C under reduced pressure to allow for the evaporation of acetone as well as concentrating the prepared dispersion to 25 ml.

² full factorial design was employed to assess the effects of changing QRC amounts and the type of surfactant used on particle size, zeta potential, and entrapment efficiency. Two different surfactants were used namely tween 80 and poloxamer 188 with two different QRC amounts which are 10 mg and 30 mg. This resulted in four different formulations stated in Table 1.

QRC loaded polymeric nanocapsules characterization. *Particle size, polydispersity index (PDI) and zeta potential.* Dynamic light scattering was employed to determine particle size, polydispersity index and zeta potential for all the prepared formulation employing Malvern Zetasizer (Malvern Instruments, Malvern, UK) at 25 °C. One ml of each formulation was diluted to a total of 10 ml using distilled water before measurements.

Encapsulation efficiency (EE)%. The amount of QRC encapsulated in all the prepared formulation were determined indirectly through analyzing the amount of unencapsulated drug³³. Two ml of each formula was centrifuged at 15,000 RPM for 2 h at 4 °C using cooling centrifuge. 100 μ l of supernatant was diluted to a total of 800 μ l using 20% ethanol in deionized water solution and measured spectrophotometrically at $\lambda_{\text{max}} = 367$ nm using UV spectrophotometer. EE% was calculated using the following equation:

$$EE\% = \frac{W_{\text{initial}} - W_{\text{free}}}{W_{\text{initial}}}$$

where W_{initial} is the initial amount of the drug used and W_{free} is the amount of drug present in the supernatant³⁴.

Based on the previous characterization techniques, the best formulation will be chosen. The following characterization techniques are done for the chosen formulation.

Formula	QRC (mg)	Tween 80 (mg)	Poloxamer 188 (mg)
F1	10	80	–
F2	10	–	80
F3	30	80	–
F4	30	–	80

Table 1. Different polymeric nanocapsules formulations prepared.

Transmission electron microscopy (TEM). Morphological evaluation of the chosen formula was evaluated using TEM (JTEM-1010, JEOL, Tokyo, Japan) utilizing negative staining technique. One drop of the chosen formula was placed on a carbon film covered copper grid. Uranyl acetate solution (2% w/v) was added drop wise onto the grid followed by sample drying by air at room temperature. TEM investigations were done at 80 kV.

Differential scanning calorimetry (DSC). Thermal behavior of QRC, PCL, Capryol 90, physical mixture of QRC, PCL and Capryol 90 in the ratio used in the preparation of polymeric nanocapsules which is 3:10:9 and the chosen formula were analyzed using DSC (DSC-50; Shimadzu, Kyoto, Japan). First, the chosen formula was lyophilized using freeze dryer (Alpha 1-2LD plus; Christ, Osterode am Harz, Germany) at -45°C for 14 h. Second, accurately weighed amount of each sample was sealed in an aluminum pan. The pan was heated from 30 to 400°C with a rate of $10^{\circ}\text{C}/\text{min}$ under nitrogen atmosphere. The data were analyzed using TA-50 WSI thermal analyzer (Shimadzu, Kyoto, Japan).

X-Ray diffraction (XRD). Crystalline or amorphous properties of QRC, PCL, physical mixture of QRC and PCL in the ratio used in the preparation of polymeric nanocapsules which is 3:10 and the chosen formula were evaluated using X-ray diffractometer (D8; Bruker Co., Germany). The scanned diffraction angle 2θ ranged from 5° to 90° with a scan rate of $1^{\circ}/\text{min}$.

In vitro release study. *In vitro release of unencapsulated QRC and QRC loaded polymeric nanocapsules.* Dialysis bag technique was used to evaluate the in vitro release of the chosen QRC loaded polymeric nanocapsules formulation and compare it to QRC dispersion in deionized water. One ml of the chosen formula and one ml of QRC dispersion containing equivalent amount of QRC were placed in tightly sealed dialysis bag (molecular weight cutoff 12,000–14,000). The dialysis bags were placed in 100 ml beakers comprising 50 ml phosphate buffer saline pH 7.4 containing 1% tween 80 as the release media. The beakers were placed in a shaking water bath set at $37 \pm 0.5^{\circ}\text{C}$ and 50 RPM for 48 h. One ml sample of the release media was withdrawn at 0.5, 1, 2, 3, 4, 5, 6, 24, and 48 h. The withdrawn volume was compensated with fresh release media maintaining the same final volume and the sink condition through the entire experiment. The withdrawn samples were analyzed spectrophotometrically at $\lambda_{\text{max}} = 367\text{ nm}$. The obtained absorbances were used to calculate cumulative QRC release percentage.

In vitro release kinetics. Release kinetics of free QRC and QRC loaded polymeric nanocapsules was analyzed through fitting the in vitro release data onto different mathematical models namely zero order, first order, Higuchi, and Hixson–Crowell. In order to identify QRC release mechanism from the polymeric nanocapsules, Korsmeyer–Peppas model was employed. The release kinetics were obtained using DDSolver software, a menu-driven add-in program for Microsoft Excel. After fitting the experimental data, adjusted r^2 was used as a model selection criterion.

Animal studies. *Animals.* Adult female Sprague Dawley rats ($n=20$, weight 250–310 gm, 11 weeks old) bred at the Faculty of Pharmacy, the British University in Egypt animal house were caged at standard plastic cages (5 per cage). The rats were kept under standard conditions of temperature ($25 \pm 0.5^{\circ}\text{C}$), relative humidity ($55 \pm 1\%$) and light cycle (12 h light and 12 h dark) with free access to food and water. Dedicated efforts were made to minimize animal suffering. All animal work was carried out according to the National Institutes of Health guide for the care and use of laboratory animals and approved by the Ethical Committee of Faculty of Pharmacy, the British University in Egypt with the ethical approval number: EX-2209. The methods are reported in accordance with Arrive guidelines.

Experimental design. The experiment is a single dose, one-way study design. Rats were simply randomized into four groups ($n=5$); control group administered saline intranasally, oral QRC dispersion, intranasal QRC dispersion, intranasal QRC loaded polymeric nanocapsules. Oral QRC dispersion group received QRC dispersed in deionized water. Oral dose was 50 mg/kg using oral gavage which was previously reported to exert anxiolytic effect³⁵. Intranasal QRC dispersion, and intranasal QRC polymeric nanocapsules groups received 35 μl dispersion containing 0.15 mg/kg QRC. The intranasal dose was administered via a micropipette directly into the rats' nostril.

Behavioral assessment. Rats' behavior was assessed for their anxiety and cognitive effect using open field test and elevated plus-maze test after single administration. Behavioral assessment started 30 min after administering the intranasal dose and 150 min after administering the oral dose. The difference in time between the oral and intranasal route was established to allow time for the oral QRC to be absorbed through the gastrointestinal tract.

Open field test. Black plexiglas box ($58 \times 58 \times 39\text{ cm}$) was used to conduct the open field test. The test was conducted in the light period of the day in a silent room in the laboratory. Animals were placed in the center of the field and videotaped for 5 min. The field was wiped thoroughly using ethanol between each session. Videos were analyzed using ANY-maze video tracking software (Stoelting co., Illinois, USA) for time spent in the center of the field while having the data analyst not aware of the groups' allocation.

Elevated plus-maze test. Standard black wooden apparatus, consist of four arms, elevated 49 cm of the ground was used for the elevated plus-maze test. The four arms were two opposite open arms (49 × 9 cm), and two opposite enclosed arms (49 × 9 × 30 cm) each placed perpendicularly relative to the adjacent arm forming a plus sign. The arms were connected using a center stage (10 × 10 cm). The test was conducted in the light period of the day in a silent room in the laboratory. Animals were placed on the center stage facing an enclosed arm and videotaped for 5 min. The field was wiped thoroughly using ethanol between each session. Videos were analyzed using ANY-maze video tracking software (Stoelting co., Illinois, USA) for the time spent in the open arms while having the data analyst not aware of the groups' allocation.

Safety studies. Observational nasal irritation test. During nasal administration conducted in animal studies, an observational nasal irritation test was conducted³⁶. Visual observation was conducted when saline, QRC dispersion, and QRC loaded polymeric nanocapsules were administered intranasally. The animals were carefully monitored for signs of mucosal inflammation including discomfort, sneezing, and itching. The nasal mucosa irritation index reported by Elnaggar et al. was employed³⁷. The index identifies four degrees of irritation according to percentage of animals showing irritation signs. These degrees are strong irritation (more than 60% of the animals), moderate irritation (from 30 to 60%), mild irritation (from 10 to 30%), and no irritation (up to 10%).

Histopathological examination. In order to investigate the nasal mucosa toxicity of the chosen formula, Histopathological evaluation was conducted following the procedure reported by Abou Youssef et al.³⁸ with slight modification. Adult female Sprague Dawley rats (n = 6, weight 250–310 gm, 11 weeks old) were randomly distributed into 3 groups (n = 2); negative control group that received 35 µl saline, positive control group which received 35 µl of 0.2% benzalkonium chloride solution, and treatment group that received 35 µl of the chosen formula in a single nostril. Animals were sacrificed 20 min post intranasal administration and the nasal mucosa were carefully harvested and stored in 10% formalin solution. Rats were euthanized using a carbon dioxide system. Rats were placed in the carbon dioxide chamber for 3–5 min. Heartbeat and respiratory symptoms were carefully monitored after the rats' removal from the chamber to confirm their absence. This was followed by cervical dislocation. The samples were embedded in paraffin, cut into four µm-thick sections, then stained using hematoxylin and eosin (H&E) for investigation using light microscope to detect any damage in the nasal mucosa.

Statistical analysis. Data were analyzed by one-way analysis of variance (one-way ANOVA) followed by Tukey–Kramer post hoc statistical tests and presented as mean ± standard deviation (SD). The analysis was done using GraphPad Prism (V9) (GraphPad Software, San Diego, CA, USA). Values of P < 0.05 were considered to be statistically significant.

Ethics approval. All institutional and national guidelines for the care and use of laboratory animals were followed. All animal work was approved by the Ethical Committee of Faculty of Pharmacy, the British University in Egypt with the ethical approval number: EX-2209.

Results

Theoretical screening of QRC solubility in different liquid lipids. In order to select the best possible liquid lipid to solubilize QRC, theoretical screening was employed using HSP. The Euclidean distance between QRC and the different liquid lipids alongside the parameters of all materials are mentioned in Table 2 Each mate-

Material	δ_D	δ_P	δ_H	Euclidean distance
QRC	21	10.6	13.7	–
Capryol 90	16.39	4.98	8.41	8.99
Capryol PGMC	16.33	4.46	7.19	10.09
Labrafil M 1944 CS	16.27	3.63	6.64	10.99
Labrafil M 2125 CS	16.17	3.69	6.19	11.3
Oleic Acid	16.4	3	5.5	12.09
Captex 200P	16.23	2.99	4.04	13.19
Labrafac PG	16.25	2.83	3.92	13.36
Labrafac Lipophile WL 1349	16.42	3.06	3.58	13.43
Miglyol 810	16.43	2.99	3.51	13.51
Captex 355	16.45	2.83	3.38	13.7
Ethyl oleate	16.1	2.3	2.90	14.48
Isopropyl myristate	15.9	2.1	2.80	14.73

Table 2. HSP of QRC and different liquid lipids as well as the Euclidean distance between QRC and each liquid lipid.

rial using its parameters is plotted in a 3D diagram (Fig. 1) using Matlab version 2021a (Mathworks, Inc., Natick, MA, USA) to visualize the distance between QRC and each liquid lipid.

Among the different liquid lipids assessed, Capryol 90 exhibited the lowest Euclidean distance while isopropyl myristate showed the highest Euclidean distance.

Solubility study. The solubility of QRC in Capryol 90 was validated experimentally. QRC demonstrated high solubility in Capryol 90 with a value of 28.41 ± 8.91 mg/g. This value was in accordance with what was previously obtained by Pageni et al.³⁹.

QRC loaded polymeric nanocapsules characterization. Characterization is considered to be one of the critical steps in order to identify the physicochemical properties of the prepared nanoparticles⁴⁰. The results of the prepared formulations are summarized in Table 3.

All the prepared nanocapsules demonstrated a size in the nano scale ranging from 184.6 nm for F1 to 278.1 nm for F4. PDI values ranged from 0.19 for F1 to 0.466 for F3. These PDI values indicated good homogeneity for all of the prepared formulations as it was previously reported that the ideal PDI value is less than 0.5⁴¹. Regarding zeta potential, the prepared nanocapsules exhibited values ranging from -14.1 mV for F1 to -18.7 mV for F4. All of the prepared formulations are considered to be stable as it was previously reported that zeta potential values between -15 mV and -30 mV are considered ideal for nanoparticles stabilization⁴² as well as the presence of steric stabilization⁴³. As for EE%, the values ranged between 79.1% for F1 to 92.7% for F4.

Based on these results, F3 was chosen to be subjected to further investigations.

The morphology of the chosen formula was evaluated using TEM. As shown in (Fig. 2), TEM image shows well defined, spherical shaped nanoparticles that appear to be unilamellar.

Thermal analysis of QRC, PCL, Capryol 90, physical mixture, and the chosen formula using DSC (Fig. 3). QRC displayed a sharp endothermic peak at 322 °C similar to what was previously reported by Li et al.⁴⁴. PCL displayed a sharp endothermic peak at 65.26 °C close to what was reported by González-Reza et al.⁴⁵. Capryol 90 displayed no peaks similar to what was previously reported by Ibrahim et al.⁴⁶. The physical mixture exhibited a shift in both melting peaks of PCL and QRC to lower melting points at 58.66 °C and 271.06 °C respectively. However, the chosen formula displayed a broad peak 290.3 °C with the disappearance of QRC peak and shifting of the PCL peak to 46.37 °C.

XRD was conducted for pure QRC, PCL, physical mixture, and the chosen formula (Fig. 4). QRC displayed its highly crystalline structure⁴⁷ through exhibiting sharp peaks at 2θ of 10.73° , 12.45° , 13.06° , 14.1° , 15.76° ,

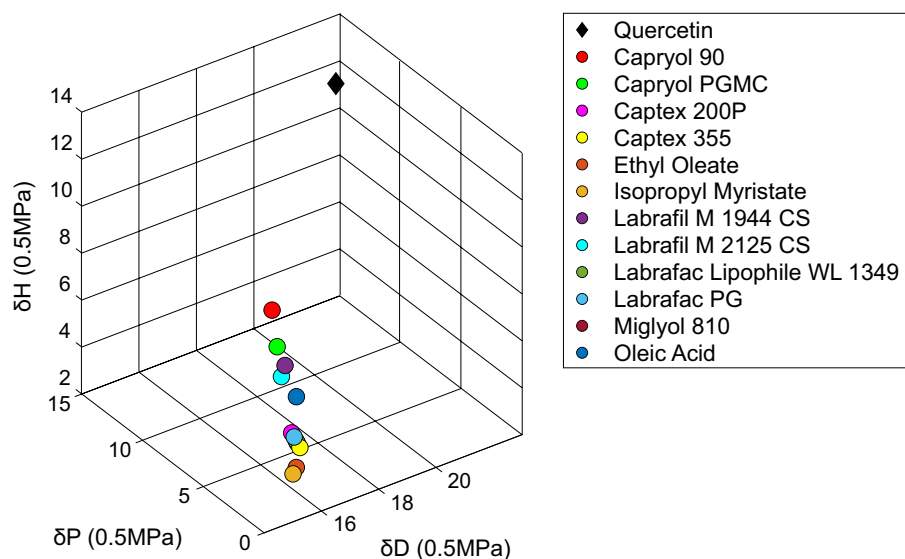


Figure 1. 3D diagram representing the Euclidean distance between QRC and the different liquid lipids.

Formula	Particle size (nm)	PDI	Zeta potential (mV)	EE%
F1	184.6 ± 4.4	0.19 ± 0.015	-14.1 ± 0.14	79.1 ± 2.3
F2	262.3 ± 1.6	0.268 ± 0.017	-15 ± 0.57	83.9 ± 1.6
F3	227.8 ± 11.9	0.466 ± 0.023	-17.5 ± 0.01	92.5 ± 1.9
F4	278.1 ± 3.7	0.371 ± 0.018	-18.7 ± 1.70	92.7 ± 2.1

Table 3. Summary of the results obtained for all the prepared formulae.

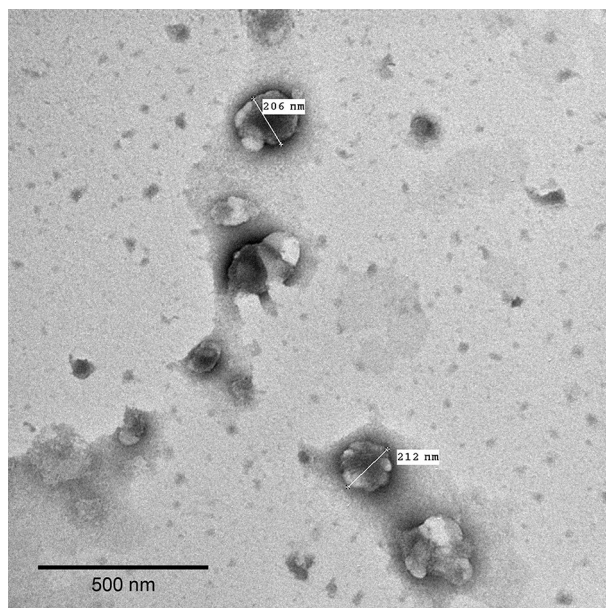


Figure 2. TEM image of F3.

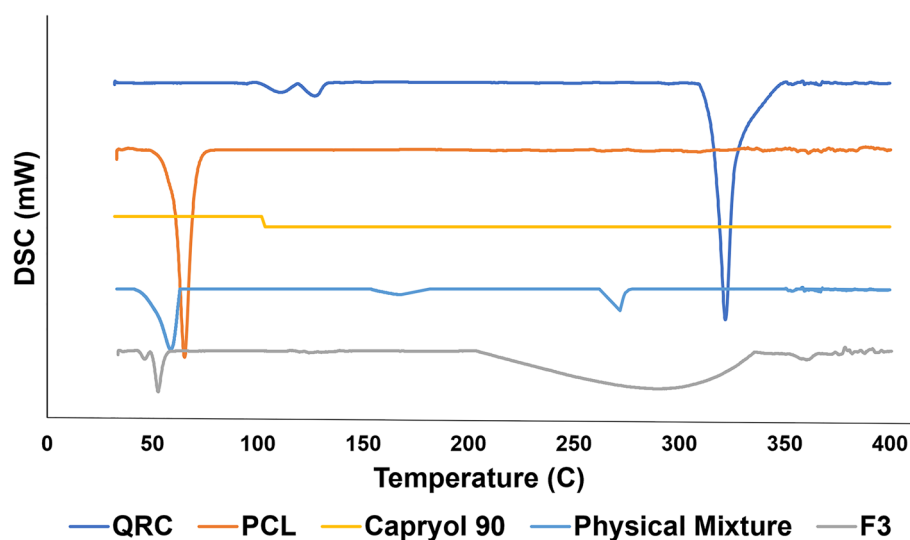


Figure 3. DSC charts of QRC, PCL, Capryol 90, physical mixture and F3.

17.16°, 22.09°, 26.49°, and 26.99°. PCL displayed its semi crystalline structure⁴⁸ by exhibiting two peaks at 21.49°, and 23.86°. The physical mixture displayed the characteristic peaks of both PCL and QRC. Albeit the low intensity of QRC peaks which may be due to the small quantity of QRC used. The chosen formula exhibited only PCL peaks with the complete disappearance of QRC peaks indicating the drug change in structure from crystalline to amorphous.

In vitro release study. Release pattern of both the chosen formulation of QRC loaded polymeric nanocapsules and QRC dispersion are illustrated in (Fig. 5). As shown in the figure, the prepared formulation resulted in a much slower release pattern over the course of the experiment compared to QRC dispersion. After 6 h, the cumulative percent release of the prepared nanocapsules was 36.06% compared to 53.91% of QRC dispersion. The release of the prepared nanocapsules continued to exhibit slower release after 24 h with cumulative release of 63.38% for the prepared nanocapsules compared to 82.71% for the QRC dispersion. In vitro release of QRC loaded polymeric nanocapsules exhibited a biphasic release with an initial burst release followed by a sustained release pattern with the release of both, the prepared nanocapsules and QRC dispersion, reaching almost complete release after 48 h.

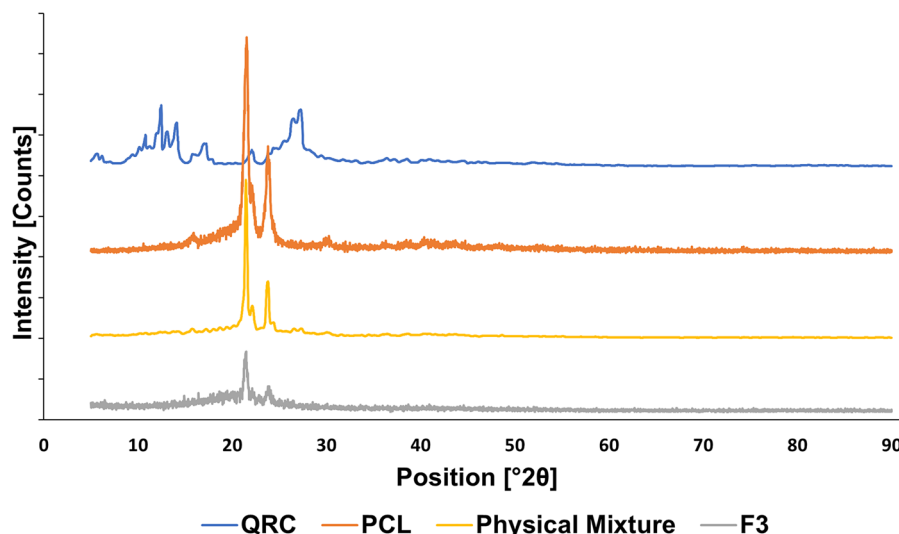


Figure 4. XRD charts of QRC, PCL, physical mixture, and F3.

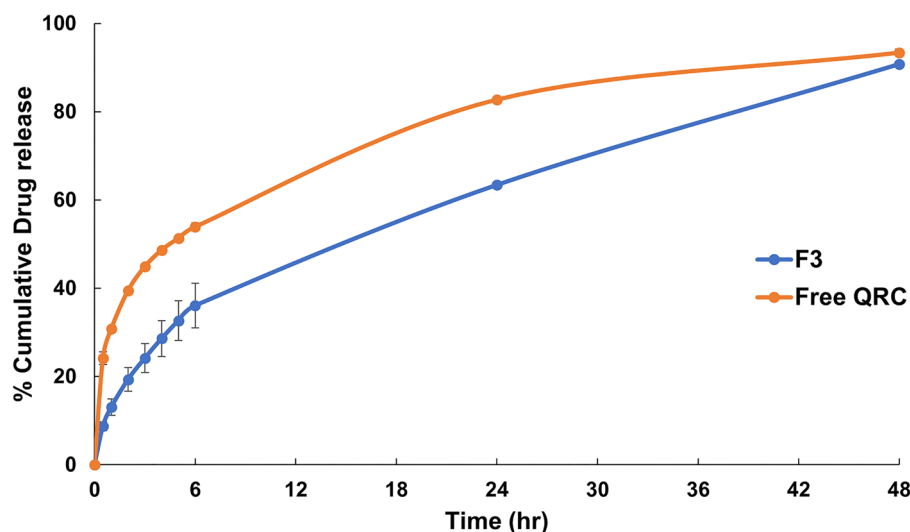


Figure 5. In vitro release profile of free QRC and F3.

Model	Equation	R ² adjusted free QRC	R ² adjusted QRC loaded polymeric nanocapsules
Zero order	$Q = Q_0 + K_0t$	-0.4732	0.3838
First order	$dC/dT = -Kt$	0.8402	0.7834
Higuchi	$Q = K_H t^{1/2}$	0.7022	0.9947
Hixson-Crowell	$Q_0^{1/3} - Q_t^{1/3} = K_{HC} t$	0.5805	0.6777

Table 4. Summary of different release models and the corresponding r^2 adjusted. Q is the amount of drug released or dissolved, Q_0 is the initial amount of drug in solution, t is time, K_0 is the zero order release constant, dC is the concentration derivative, dT is the time derivative, K is the first order rate constant, K_H is the Higuchi dissolution rate constant, Q_t is the remaining weight of solid at time t, K_{HC} is the Hixson-Crowell dissolution rate constant.

Through analyzing the kinetic models applied to the release data of free QRC and QRC loaded polymeric nanocapsules (Table 4), it was possible to determine that the release profile of free QRC followed first order model (r^2 adjusted = 0.8402). While the release profile of QRC loaded polymeric nanocapsules followed Higuchi model (r^2 adjusted = 0.9947). The n value of Korsmeyer–Peppas model for free QRC was 0.316 with a r^2 adjusted of 0.9983 while the n value for QRC loaded polymeric nanocapsules was 0.48 with a r^2 adjusted of 0.9957.

Animal studies. The anxiolytic effect was assessed by two behavioral assessments which are open field and elevated plus-maze. The results of both assessments are present in (Fig. 6). When analyzing the open field results, intranasal QRC loaded polymeric nanocapsules significantly increased the time spent in the center of the field compared to the control group ($P < 0.05$), oral QRC dispersion group ($P < 0.05$), and intranasal QRC dispersion ($P < 0.05$).

Regarding elevated plus-maze, intranasal QRC loaded polymeric nanocapsules significantly increased the time spent in the open arms compared to the control group ($P < 0.05$), oral QRC dispersion group ($P < 0.01$), and intranasal QRC dispersion ($P < 0.01$).

Safety studies. In order to ensure the safety of our prepared formulation, safety studies were conducted using both observational nasal irritation test and histopathological examination. Visual observation demonstrated that the animals administered intranasally with both, QRC loaded polymeric nanocapsules as well as QRC dispersion, did not exhibit any signs of nasal mucosal irritation compared to animals administered with intranasal saline. This resulted in classifying both QRC loaded polymeric nanocapsules as well as QRC dispersion in the no irritation level on the nasal mucosa irritation index.

Histopathological examination of the negative control group showed intact epithelial lining, average sub-mucosa with average blood vessels and cellularity, and average nasal cartilage. While the positive control group demonstrated ulcerated epithelial lining, submucosa with marked hypercellularity, marked inflammatory infiltrate, and marked edema. Regarding our chosen formula, histopathological examination revealed intact epithelial lining, submucosa with average cellularity, average nasal cartilage, and minute edema compared to the positive control group (Fig. 7).

Discussion

In this study polymeric nanocapsules incorporating QRC were prepared using PCL and Capryol 90. The effect of varying the initial amount of QRC as well as the type of surfactant used was evaluated in order to identify the best formula. The best formula was characterized using multiple characterization techniques. The best formula was also evaluated in vivo using two behavioral tests to assess the anxiolytic effect utilizing the intranasal route.

Nanocapsules are characterized by the presence of an inner core surrounded by an outer polymeric shell. Formulating an efficient drug delivery system depends on the accurate selection of the contributing materials⁴⁹.

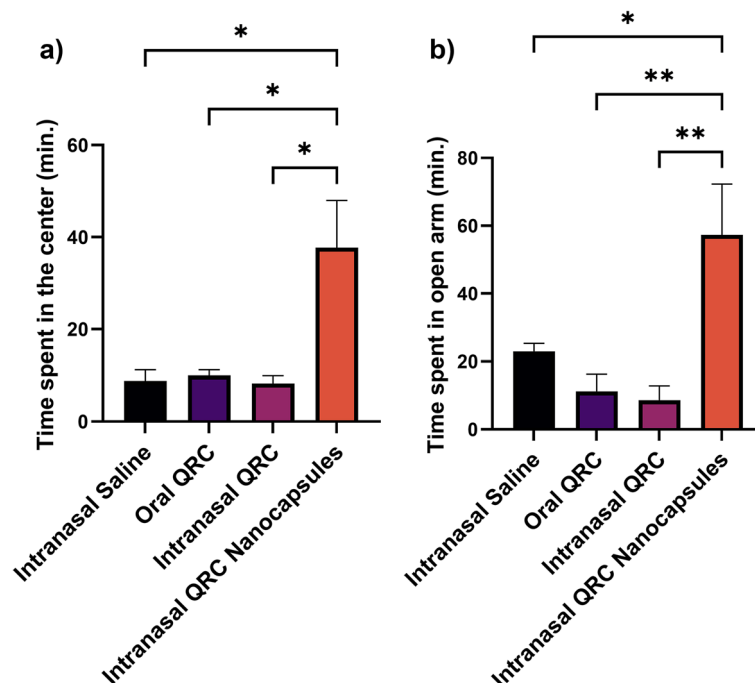


Figure 6. In vivo results of (a) time spent in the center of the open field, and (b) time spent in the open arm of the elevated plus-maze. The vertical bars represent mean \pm Standard Error of Mean (SEM) where values are statistically significant at $P < 0.05$. * $P < 0.05$, ** $P < 0.01$.

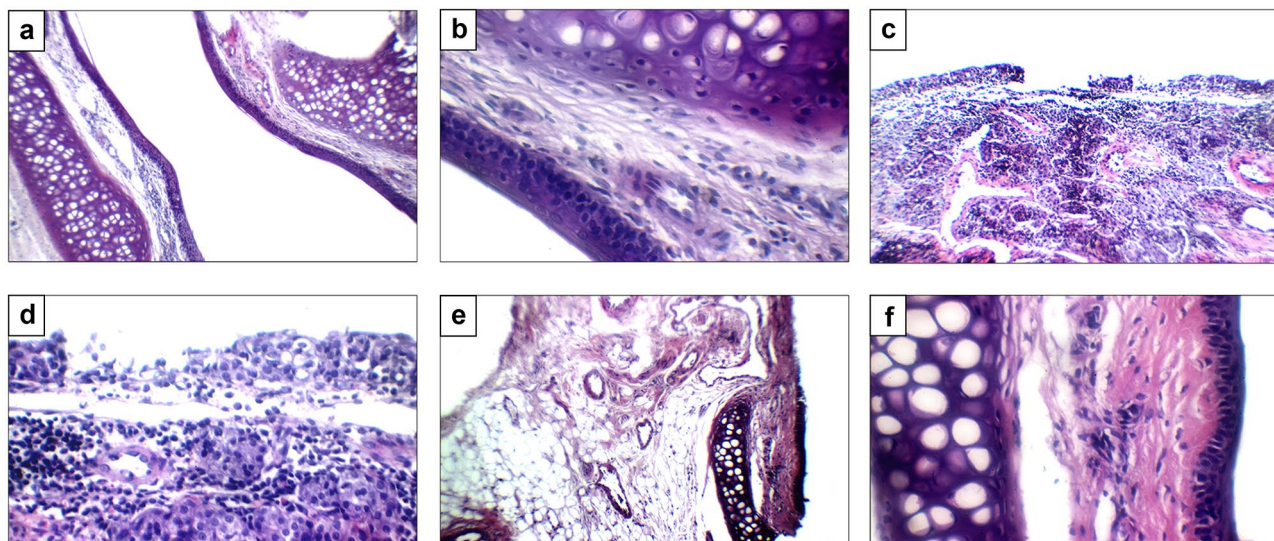


Figure 7. Histopathological examination of nasal mucosa of rats receiving saline at (a) $\times 200$ and (b) $\times 400$, benzalkonium chloride at (c) $\times 200$ and (d) $\times 400$, and F3 at (e) $\times 200$ and (f) $\times 400$.

PCL was chosen as the polymeric outer shell as a result of its advantages including biodegradability, and lack of toxicity⁵⁰. Multiple options exist regarding the choice of an oily core to entrap hydrophobic active ingredients. The most important factor is the solubility of the active pharmaceutical ingredient in the chosen oil as higher solubility results in higher EE%⁵¹. HSP were used to predict the solubility between QRC and different liquid lipids. HSP are based on the concept that the total cohesive energy can be divided into three main parts. δ_D which refers to dispersion forces (van der Waals), δ_P that refers dipole forces (polarity), and δ_H which refers to hydrogen bonding. The sum of squares of these three parameters results in the square of Hildebrand (total solubility parameter [Eq. (2)]⁵².

$$\delta^2 = \delta^2D + \delta^2P + \delta^2H \quad (2)$$

Euclidean distance is used to predict solubility, higher solubility is obtained with smaller distance. The smaller the distance, the higher the affinity between the solute and solvent, hence higher solubility⁵⁰. Among the tested liquid lipids, Capryol 90 exhibited the lowest euclidean distance, thus, the highest solubilizing power for QRC. This inference was validated by previous solubility testing conducted for QRC available in the literature^{39,53} where Capryol 90 (propylene glycol monocaprylate) and propylene glycol displayed the highest solubility for QRC. The solubilization power of Capryol 90 for QRC was also determined experimentally. The high solubility obtained of 28.41 ± 8.91 mg/g indicates the high solubilizing power of Capryol 90. Hence, Capryol 90 was chosen as the liquid lipid.

QRC loaded polymeric nanocapsules were prepared using a modified nanoprecipitation method. In our study, the obtained particle sizes are similar to the particle sizes obtained by dos Santos et al.⁵⁴ and Joo et al.⁵⁵. Changing the amounts of QRC and the type of surfactant used exhibited varying effects of particle size and PDI. When tween 80 was used as a surfactant, the particle size increased from 184.6 to 227.8 nm when QRC amounts changed from 10 to 30 mg. The same effect was observed with poloxamer 188 as the surfactant where the particle size increased from 262.3 with 10 mg QRC to 278.1 nm with 30 mg QRC. These results are in accordance with the results reported by Pegoraro et al. where increasing the amount of vitamin E encapsulated in PCL nanocapsules resulted in an increase in the particle size⁵⁶. It is also evident the particle size increased when poloxamer was used instead of tween 80 with both amounts of QRC. It was reported by El-Gogary et al. that tween 80 is characterized by higher adsorption potential compared to poloxamer 407 resulting in smaller particle sizes when tween 80 was used⁵⁷. Regarding PDI, increasing QRC amounts from 10 to 30 mg decreased the homogeneity of sample resulting in higher PDI. Similar observations were reported by Araújo et al. when increasing the amount of cloxacillin benzathine in PCL nanocapsules⁵⁸.

Zeta potential is defined as the effective electric charge on the surface of nanoparticles and is considered one of the main parameters that indicate stability⁵⁹. In our study, all formulations exhibited negative zeta potential values which can be attributed to the dissociation of the carboxylic group of PCL. This dissociation result in the presence of the polar groups of PCL on the surface of the nanocapsules leading to negative zeta potential values⁶⁰. Our prepared formulations exhibited zeta potential values similar to these reported by Zambrano-Zaragoza et al.⁶¹. The absolute values of zeta potential are expectedly relatively low -despite being in the stable range- as a result of the presence of non-ionic surfactants. It was reported by Sis et al. that the presence of non-ionic surfactants decreases the magnitude of zeta potential on a wide range of pH ranging between 3.0 and 11.0⁶². The other form of stabilization as a result of the presence of non-ionic surfactants is steric stabilization. Steric stabilization is the process by which the adsorbed non-ionic surfactants produce strong repulsion between the particles when the adsorbed layer is hydrated by the molecules of the solvent⁴³.

EE% represents the amount of the active constituent encapsulated in the nanoparticles. EE% achieved in our study is similar to the results reported by Ibrahim et al.⁶³. The high amount of QRC encapsulated in all the prepared formulations can be attributed to the high solubility of QRC in Capryol 90. It was previously reported that high solubility of the active constituent in oils can result in higher EE%³⁰. Upon changing QRC amounts from 10 to 30 mg, the EE% increased from 79.1 and 83.9% to 92.5 and 92.7%. This increase in EE% suggest the high capability of the chosen system -both PCL and Capryol 90- to solubilize QRC in large amounts as it was previously reported that encapsulation efficiency depend on the active constituent miscibility in both polymer and lipid^{64,65}. Ersoz et al. reported similar findings were the encapsulation efficiency of QRC increased with increasing QRC initial amount⁶⁶. Among the four prepared formulations, F3 was chosen as the best formulation. This choice was made based on the fact that this formula possessed small particle size, high entrapment efficiency, comparable zeta potential to the remaining formulations, and acceptable PDI. All the following experimental procedure was done on the F3.

The chosen formula exhibited spherical, unilamellar, and well-defined nanoparticles when evaluated using TEM. This was in accordance with what was previously reported by Ibrahim et al.⁶³.

In order to analyze the thermal behavior of QRC, PCL, Capryol 90, physical mixture and F3, DSC analysis was conducted. The results have shown the presence of a sharp endothermic peak for both QRC and PCL. When analyzing the results of the physical mixture, it was evident that both PCL and QRC peaks shifted toward lower melting points. The shift in PCL melting point in the physical mixture suggests the homogenous mixing of the polymer and oil⁶⁷. The shift in QRC melting point confirms the ability of Capryol 90 to solubilize QRC which resulted in an earlier QRC melting. The chosen formula demonstrated a peak shift from 58.66 to 46.37 °C which suggests a closer component interaction because of the formation of nanoparticles. Also, the QRC peak disappeared, and a new broad peak appeared. This disappearance indicates successful encapsulation of the active ingredient into nanoparticles^{68,69}. These results are in accordance with what was previously reported by Penteado et al. where the melting peak of perillyl alcohol disappeared after its incorporation in chitosan coated PCL nanocapsules⁷⁰.

The nature of the structure of QRC, PCL, physical mixture and F3 whether crystalline or amorphous was analyzed using XRD. QRC exhibited highly crystalline structure while PCL demonstrated semi-crystalline structure. The mixture of PCL and QRC demonstrated the characteristic peaks of both. However, there was a complete disappearance of QRC peaks in F3. This can be explained by a change in the structure of QRC from crystalline to amorphous during the nanocapsules preparation. This indicates the incorporation of QRC in the prepared nanoparticles⁷¹. Similar findings were reported by Carletto et al. when resveratrol peaks disappeared after its incorporation in PCL nanocapsules⁷².

QRC loaded polymeric nanocapsules were able to provide much lower release for QRC compared to free QRC while modifying the release kinetics of QRC. The prepared polymeric nanocapsules were able to modify the release kinetics of QRC from first order model to Higuchi model as well as the n value of Korsmeyer–Peppas model from 0.316 to 0.48. The release pattern of QRC loaded polymeric nanocapsules exhibited biphasic pattern with initial burst release followed by a sustained release pattern. This pattern was previously reported when preparing polymeric nanoparticles using nanoprecipitation method⁷³. The initial burst release can be attributed to the desorption of the active ingredient from the surface of the nanocapsules and/or the release of active molecules present near the surface of the nanocapsules. The second sustained release occur as a result of the active ingredient diffusion through the nanocapsules and erosion of the polymeric shell⁷⁴. This was further confirmed by the release kinetics analysis. It was determined that Higuchi's diffusion model is the release kinetics model of the prepared QRC loaded polymeric nanocapsules since Higuchi model had the highest adjusted r² value. Regarding Korsmeyer–Peppas model, it was previously reported that in case of spherical geometry, n value between 0.43 and 0.85 indicates that the release mechanism is governed by both diffusion and polymer erosion mechanisms⁷⁵. The n value of our formulation was 0.48 indicating QRC release by both mechanisms as previously mentioned. This may indicate that QRC diffuse through the prepared nanocapsules after the degradation of thin polymeric outer layer. This was in accordance with what was previously mentioned by Abdel-Rashid et al.⁷⁶. It is also worth mentioning that both QRC loaded polymeric nanocapsules and QRC dispersion almost reached complete release at the end of the experiment indicate the successful attainment of the sink condition and the availability of the active ingredient transfer to the release media without limitations⁷⁷.

The next step is the in vivo evaluation of the chosen formula administered intranasally. Behavioral assessment was used to assess the anxiolytic effect of QRC loaded polymeric nanocapsules compared to control group, oral QRC dispersion and intranasal QRC dispersion. Two behavioral assessments were used as anxiety models which are open field and elevated plus-maze. Rats placed in foreign environment (open field and elevated plus-maze) either spend time in relative safety (near the walls of the open field, and in the closed arms of the elevated plus-maze) or explore dangerous area (center of the open field, and in the open arms of the plus-maze). Anxiolytic activity is determined by higher tendency of the rats to explore dangerous areas⁷⁸.

The highest anxiolytic effect obtained from behavioral testing was achieved when the intranasal route was utilized in administering the prepared QRC loaded polymeric nanocapsules. All the parameters analyzed in both behavioral assessments indicated that intranasal QRC loaded polymeric nanocapsules significantly improved the assessed parameters resulted in the best anxiolytic effect. These results are in accordance with what was previously reported by Pripem et al.¹⁷.

Improvements in QRC anxiolytic effects observed with the encapsulation of QRC in polymeric nanocapsules administered intranasally is most likely due to the improved QRC delivery to the brain which can be attributed to the ability of nanoparticles to directly deliver therapeutics to the brain when administered intranasally. Although this inference is well supported in the available literature^{79–81}, further validation might be required to confirm the improved accumulation of QRC in the brain experimentally.

Ensuring the safety of any prepared formulation is paramount in any pharmaceutical development process. Our prepared formulation as well as QRC dispersion demonstrated no signs of nasal irritation when administered intranasally compared to when saline was administered intranasally. Based on these observations, both QRC loaded polymeric nanocapsules as well as QRC dispersion were placed in the no irritation level on the nasal mucosa irritation index indicating that both are cilio-friendly³⁶. To further validate the safety of our chosen formula, histopathological examination was conducted to analyze the rats' mucosa when the rats received either saline, benzalkonium chloride, or the chosen formula. Compared to rats receiving benzalkonium chloride, the rats that received our chosen formula demonstrated normal nasal mucosal structure with minute edema compared to rats receiving benzalkonium chloride indicating better tolerability and the safety of the prepared formulation.

Conclusion

The present study successfully formulated QRC loaded polymeric nanocapsules using nanoprecipitation method of preparation. Both the type of surfactant and the drug amount were used with different levels. It was evident that tween 80 produced particles with smaller size compared to these produced by poloxamer 188. It was also evident that increasing the drug amount increased the particle size as well as the EE%. The best formula was chosen and assessed for its anxiolytic effect in vivo using two behavioral tests after intranasal administration which demonstrated significant improvements in the anxiolytic effect of QRC. This improvement was achieved while showing good safety and tolerability profile. The obtained results proved that encapsulating QRC in polymeric nanocapsules to be administered intranasally is a promising and successful strategy to improve the anxiolytic effect of QRC.

Data availability

The datasets used and/or analyzed during the current study are available from the corresponding author on reasonable request.

Received: 30 August 2022; Accepted: 5 January 2023

Published online: 10 January 2023

References

- Vandebos, G. *APA Dictionary of Psychology* (American Psychological Association, 2007).
- GBD 2019 Mental Disorders Collaborators. Global, regional, and national burden of 12 mental disorders in 204 countries and territories, 1990–2019: A systematic analysis for the Global Burden of Disease Study 2019. *Lancet Psychiatry* **9**, 137–150 (2022).
- Santomauro, D. F. *et al.* Global prevalence and burden of depressive and anxiety disorders in 204 countries and territories in 2020 due to the COVID-19 pandemic. *Lancet* **398**, 1700–1712 (2021).
- Craske, M. G. *et al.* Anxiety disorders. *Nat. Rev. Dis. Prim.* **3**, 17024 (2017).
- Bandelow, B., Michaelis, S. & Wedekind, D. Treatment of anxiety disorders. *Dialog. Clin. Neurosci.* **19**, 93–107 (2017).
- Garakani, A. *et al.* Pharmacotherapy of anxiety disorders: Current and emerging treatment options. *Front. Psychiatry* **11**, 5584 (2020).
- Fajemiroye, J. O., da Silva, D. M., de Oliveira, D. R. & Costa, E. A. Treatment of anxiety and depression: Medicinal plants in retrospect. *Fundam. Clin. Pharmacol.* **30**, 198–215 (2016).
- Leitzmann, C. Characteristics and health benefits of phytochemicals. *Complement. Med. Res.* **23**, 69–74 (2016).
- Kosari-Nasab, M., Shokouhi, G., Ghorbanihaghjo, A., Mesgari-Abbasi, M. & Salari, A.-A. Quercetin mitigates anxiety-like behavior and normalizes hypothalamus–pituitary–adrenal axis function in a mouse model of mild traumatic brain injury. *Behav. Pharmacol.* **30**, 282–289 (2019).
- Islam, M. S. *et al.* Anxiolytic-like effect of quercetin possibly through GABA receptor interaction pathway: In vivo and in silico studies. *Molecules* **27**, 7149 (2022).
- Salehi, B. *et al.* Therapeutic potential of quercetin: New insights and perspectives for human health. *ACS Omega* **5**, 11849–11872 (2020).
- Silvestro, S., Bramanti, P. & Mazzon, E. Role of quercetin in depressive-like behaviors: Findings from animal models. *Appl. Sci.* **11**, 7116 (2021).
- da Silva, W. M. B. *et al.* Synthesis of quercetin–metal complexes, in vitro and in silico anticholinesterase and antioxidant evaluation, and in vivo toxicological and anxiolytic activities. *Neurotox. Res.* **37**, 893–903 (2020).
- Kim, J. & Wessling-Resnick, M. Iron and mechanisms of emotional behavior. *J. Nutr. Biochem.* **25**, 1101–1107 (2014).
- Lesjak, M. *et al.* Quercetin inhibits intestinal iron absorption and ferroportin transporter expression in vivo and in vitro. *PLoS ONE* **9**, e102900 (2014).
- Merzoug, S., Toumi, M. L. & Tahraoui, A. Quercetin mitigates adriamycin-induced anxiety- and depression-like behaviors, immune dysfunction, and brain oxidative stress in rats. *Naunyn. Schmiedeberg's Arch. Pharmacol.* **387**, 921–933 (2014).
- Priprem, A., Watanatorn, J., Sutthiparinyanont, S., Phachonpai, W. & Muchimapura, S. Anxiety and cognitive effects of quercetin liposomes in rats. *Nanomed. Nanotechnol. Biol. Med.* **4**, 70–78 (2008).
- Li, Y. *et al.* Quercetin, inflammation and immunity. *Nutrients* **8**, 167 (2016).
- Jeevanandam, J., Barhoum, A., Chan, Y. S., Dufresne, A. & Danquah, M. K. Review on nanoparticles and nanostructured materials: History, sources, toxicity and regulations. *Beilstein J. Nanotechnol.* **9**, 1050–1074 (2018).
- Rishitha, N. & Muthuraman, A. Therapeutic evaluation of solid lipid nanoparticle of quercetin in pentylenetetrazole induced cognitive impairment of zebrafish. *Life Sci.* **199**, 80–87 (2018).
- Tong-Un, T., Wannanon, P., Wattanathorn, J. & Phachonpai, W. Quercetin liposomes via nasal administration reduce anxiety and depression-like behaviors and enhance cognitive performances in rats. *Am. J. Pharmacol. Toxicol.* **5**, 80–88 (2010).
- Dhawan, S., Kapil, R. & Singh, B. Formulation development and systematic optimization of solid lipid nanoparticles of quercetin for improved brain delivery. *J. Pharm. Pharmacol.* **63**, 342–351 (2011).
- Mahmoud, K., Swidan, S., El-Nabarawi, M. & Teaima, M. Lipid based nanoparticles as a novel treatment modality for hepatocellular carcinoma: A comprehensive review on targeting and recent advances. *J. Nanobiotechnol.* **20**, 109 (2022).
- Zielińska, A. *et al.* Polymeric nanoparticles: Production, characterization, toxicology and ecotoxicology. *Molecules* **25**, 1–10 (2020).
- Deng, S., Gliobianco, M. R., Censi, R. & Di Martino, P. Polymeric nanocapsules as nanotechnological alternative for drug delivery system: Current status, challenges and opportunities. *Nanomaterials* **10**, 847 (2020).

26. Xu, J., Tao, J. & Wang, J. Design and application in delivery system of intranasal antidepressants. *Front. Bioeng. Biotechnol.* **8**, 626882 (2020).
27. Dhuria, S. V., Hanson, L. R. & Frey, W. H. II. Intranasal delivery to the central nervous system: Mechanisms and experimental considerations. *J. Pharm. Sci.* **99**, 1654–1673 (2010).
28. Alavian, F. & Shams, N. Oral and intra-nasal administration of nanoparticles in the cerebral ischemia treatment in animal experiments: Considering its advantages and disadvantages. *Curr. Clin. Pharmacol.* **15**, 20–29 (2020).
29. Thangudu, S., Cheng, F.-Y. & Su, C.-H. Advancements in the blood–brain barrier penetrating nanoplatforms for brain related disease diagnostics and therapeutic applications. *Polymers* **12**, 3055 (2020).
30. Kovačević, A. B., Müller, R. H. & Keck, C. M. Formulation development of lipid nanoparticles: Improved lipid screening and development of tacrolimus loaded nanostructured lipid carriers (NLC). *Int. J. Pharm.* **576**, 118918 (2020).
31. Piazzini, V. *et al.* Nanoemulsion for improving solubility and permeability of Vitex agnus-castus extract: Formulation and in vitro evaluation using PAMPA and Caco-2 approaches. *Drug Deliv.* **24**, 380–390 (2017).
32. Elhesaisy, N. & Swidan, S. Trazodone loaded lipid core poly (ϵ -caprolactone) nanocapsules: Development, characterization and in vivo antidepressant effect evaluation. *Sci. Rep.* **10**, 1964 (2020).
33. Chalikwar, S. S., Belgamwar, V. S., Talele, V. R., Surana, S. J. & Patil, M. U. Formulation and evaluation of Nimodipine-loaded solid lipid nanoparticles delivered via lymphatic transport system. *Colloids Surf. B Biointerfaces* **97**, 109–116 (2012).
34. Wang, S. *et al.* Emodin loaded solid lipid nanoparticles: Preparation, characterization and antitumor activity studies. *Int. J. Pharm.* **430**, 238–246 (2012).
35. Toumi, M. L., Merzoug, S., Baudin, B. & Tahraoui, A. Quercetin alleviates predator stress-induced anxiety-like and brain oxidative signs in pregnant rats and immune count disturbance in their offspring. *Pharmacol. Biochem. Behav.* **107**, 1–10 (2013).
36. Abbas, H. *et al.* Novel luteolin-loaded chitosan decorated nanoparticles for brain-targeting delivery in a sporadic Alzheimer's disease mouse model: Focus on antioxidant, anti-inflammatory, and amyloidogenic pathways. *Pharmaceutics* **14**, 1003 (2022).
37. Elnaggar, Y. S. R., Etman, S. M., Abdelmonsif, D. A. & Abdallah, O. Y. Intranasal piperine-loaded chitosan nanoparticles as brain-targeted therapy in Alzheimer's disease: Optimization, biological efficacy, and potential toxicity. *J. Pharm. Sci.* **104**, 3544–3556 (2015).
38. Youssef, N. A. H. A. *et al.* A novel nasal almotriptan loaded solid lipid nanoparticles in mucoadhesive in situ gel formulation for brain targeting: Preparation, characterization and in vivo evaluation. *Int. J. Pharm.* **548**, 609–624 (2018).
39. Pangani, R., Kang, S.-W., Oak, M., Park, E. Y. & Park, J. W. Oral delivery of quercetin in oil-in-water nanoemulsion: In vitro characterization and in vivo anti-obesity efficacy in mice. *J. Funct. Foods* **38**, 571–581 (2017).
40. Barhoum, A., García-Betancourt, M. L., Rahier, H. & Van Assche, G. Physicochemical characterization of nanomaterials: polymorph, composition, wettability, and thermal stability. In *Micro and Nano Technologies* (eds Barhoum, A. & Makhlof, A. S.) 255–278 (Elsevier, 2018).
41. Rahat, I. *et al.* Thymoquinone-entrapped chitosan-modified nanoparticles: Formulation optimization to preclinical bioavailability assessments. *Drug Deliv.* **28**, 973–984 (2021).
42. Alex, A. T., Joseph, A., Shavi, G., Rao, J. V. & Udupa, N. Development and evaluation of carboplatin-loaded PCL nanoparticles for intranasal delivery. *Drug Deliv.* **23**, 2144–2153 (2016).
43. Tadros, T. Steric stabilization. In *Encyclopedia of Colloid and Interface Science* (ed. Tadros, T.) 1048–1049 (Springer, 2013).
44. Li, C., Yu, D. G., Williams, G. R. & Wang, Z. H. Fast-dissolving core-shell composite microparticles of quercetin fabricated using a coaxial electrospray process. *PLoS ONE* **9**, e92106 (2014).
45. González-Reza, R. M. *et al.* Influence of stabilizing and encapsulating polymers on antioxidant capacity, stability, and kinetic release of thyme essential oil nanocapsules. *Foods* **9**, 1884 (2020).
46. Ibrahim, T. M., Abdallah, M. H., El-Megrab, N. A. & El-Nahas, H. M. Upgrading of dissolution and anti-hypertensive effect of Carvedilol via two combined approaches: self-emulsification and liquisolid techniques. *Drug Dev. Ind. Pharm.* **44**, 873–885 (2018).
47. Wu, T. H. *et al.* Preparation, physicochemical characterization, and antioxidant effects of quercetin nanoparticles. *Int. J. Pharm.* **346**, 160–168 (2008).
48. Camargo, G. D. A. *et al.* Characterization and in vitro and in vivo evaluation of tacrolimus-loaded poly(ϵ -caprolactone) nanocapsules for the management of atopic dermatitis. *Pharmaceutics* **13**, 2013 (2021).
49. Soltani, S., Sardari, S. & Soror, S. A. Computer simulation of a novel pharmaceutical silicon nanocarrier. *Nanotechnol. Sci. Appl.* **3**, 149–157 (2010).
50. Ma, Y. *et al.* Novel docetaxel-loaded nanoparticles based on PCL-Tween 80 copolymer for cancer treatment. *Int. J. Nanomed.* **6**, 2679–2688 (2011).
51. Rapalli, V. K. *et al.* Curcumin loaded nanostructured lipid carriers for enhanced skin retained topical delivery: Optimization, scale-up, in-vitro characterization and assessment of ex-vivo skin deposition. *Eur. J. Pharm. Sci.* **152**, 105438 (2020).
52. Hansen, C. M. *Hansen Solubility Parameters: A User's Handbook, Second Edition* 2nd edn. (CRC Press, 2007).
53. Mahadev, M. *et al.* Fabrication and evaluation of quercetin nanoemulsion: A delivery system with improved bioavailability and therapeutic efficacy in diabetes mellitus. *Pharmaceutics* **15**, 1–70 (2022).
54. dos Santos, P. P. *et al.* Development of lycopene-loaded lipid-core nanocapsules: physicochemical characterization and stability study. *J. Nanoparticle Res.* **17**, 107 (2015).
55. Joo, H. H., Lee, H. Y., Guan, Y. S. & Kim, J.-C. Colloidal stability and in vitro permeation study of poly(ϵ -caprolactone) nanocapsules containing hinokitiol. *J. Ind. Eng. Chem.* **14**, 608–613 (2008).
56. Pegoraro, N. S. *et al.* Improved photostability and cytotoxic effect of coenzyme Q10 by its association with vitamin E acetate in polymeric nanocapsules. *Pharm. Dev. Technol.* **23**, 400–406 (2018).
57. El-Gogary, R. I., Gaber, S. A. A. & Nasr, M. Polymeric nanocapsular baicalin: Chemometric optimization, physicochemical characterization and mechanistic anticancer approaches on breast cancer cell lines. *Sci. Rep.* **9**, 11064 (2019).
58. Araújo, R. S. *et al.* Cloxacillin benzathine-loaded polymeric nanocapsules: Physicochemical characterization, cell uptake, and intramammary antimicrobial effect. *Mater. Sci. Eng. C* **104**, 110006 (2019).
59. Selvamani, V. Stability studies on nanomaterials used in drugs. In *Micro and Nano Technologies Mohapatra* (eds Mohapatra, S. S. *et al.*) 425–444 (Elsevier, 2019).
60. Gomes, G. S. *et al.* Optimization of curcuma oil/quinine-loaded nanocapsules for malaria treatment. *AAPS PharmSciTech* **19**, 551–564 (2018).
61. Zambrano-Zaragoza, M. L., Mercado-Silva, E., Gutiérrez-Cortez, E., Castaño-Tostado, E. & Quintanar-Guerrero, D. Optimization of nanocapsules preparation by the emulsion–diffusion method for food applications. *LWT Food Sci. Technol.* **44**, 1362–1368 (2011).
62. Sis, H. & Birinci, M. Effect of nonionic and ionic surfactants on zeta potential and dispersion properties of carbon black powders. *Colloids Surf. A Physicochem. Eng. Asp.* **341**, 60–67 (2009).
63. Ibrahim, A. H. *et al.* Lyophilized tablets of felodipine-loaded polymeric nanocapsules to enhance aqueous solubility: Formulation and optimization. *J. Drug Deliv. Sci. Technol.* **70**, 103172 (2022).
64. Panyam, J., Williams, D., Dash, A., Leslie-Pelecky, D. & Labhasetwar, V. Solid-state solubility influences encapsulation and release of hydrophobic drugs from PLGA/PLA nanoparticles. *J. Pharm. Sci.* **93**, 1804–1814 (2004).
65. Daneshmand, S. *et al.* Encapsulation challenges, the substantial issue in solid lipid nanoparticles characterization. *J. Cell. Biochem.* **119**, 4251–4264 (2018).

66. Ersoz, M., Erdemir, A., Derman, S., Arasoglu, T. & Mansuroglu, B. Quercetin-loaded nanoparticles enhance cytotoxicity and antioxidant activity on C6 glioma cells. *Pharm. Dev. Technol.* **25**, 757–766 (2020).
67. Negi, L. M., Jaggi, M. & Talegaonkar, S. Development of protocol for screening the formulation components and the assessment of common quality problems of nano-structured lipid carriers. *Int. J. Pharm.* **461**, 403–410 (2014).
68. Ortiz, A. C., Yañez, O., Salas-Huenuleo, E. & Morales, J. O. Development of a nanostructured lipid carrier (NLC) by a low-energy method, comparison of release kinetics and molecular dynamics simulation. *Pharmaceutics* **13**, 531 (2021).
69. Zhang, Y., Yang, Y., Tang, K., Hu, X. & Zou, G. Physicochemical characterization and antioxidant activity of quercetin-loaded chitosan nanoparticles. *J. Appl. Polym. Sci.* **107**, 891–897 (2008).
70. Penteado, L. *et al.* Chitosan-coated poly(ϵ -caprolactone) nanocapsules for mucoadhesive applications of perillyl alcohol. *Soft Mater.* **20**, 1–11 (2022).
71. Kurd, M., Malvajerd, S. S., Rezaee, S., Hamidi, M. & Derakhshandeh, K. Oral delivery of indinavir using mPEG-PCL nanoparticles: Preparation, optimization, cellular uptake, transport and pharmacokinetic evaluation. *Artif. Cells Nanomed. Biotechnol.* **47**, 2123–2133 (2019).
72. Carletto, B. *et al.* Resveratrol-loaded nanocapsules inhibit murine melanoma tumor growth. *Colloids Surf. B Biointerfaces* **144**, 65–72 (2016).
73. Bazylińska, U., Lewińska, A., Lamch, I. & Wilk, K. A. Polymeric nanocapsules and nanospheres for encapsulation and long sustained release of hydrophobic cyanine-type photosensitizer. *Colloids Surf. A Physicochem. Eng. Asp.* **442**, 42–49 (2014).
74. Musumeci, T. *et al.* PLA/PLGA nanoparticles for sustained release of docetaxel. *Int. J. Pharm.* **325**, 172–179 (2006).
75. Bruschi, M. L. Mathematical models of drug release. In *Strategies to Modify the Drug Release from Pharmaceutical Systems* (ed. Bruschi, M. L.) 63–86 (Woodhead Publishing, 2015).
76. Abdel-Rashid, R. S., Helal, D. A., Alaa-Eldin, A. A. & Abdel-Monem, R. Polymeric versus lipid nanocapsules for miconazole nitrate enhanced topical delivery: In vitro and ex vivo evaluation. *Drug Deliv.* **29**, 294–304 (2022).
77. Abdelbary, G. & Fahmy, R. H. Diazepam-loaded solid lipid nanoparticles: Design and characterization. *AAPS Pharm. Sci. Technol.* **10**, 211–219 (2009).
78. Rodgers, R. J. Animal tests for anxiety. In *Encyclopedia of Behavioral Neuroscience* (eds Koob, G. F. *et al.*) 90–100 (Academic Press, 2010).
79. Muntimadugu, E. *et al.* Intranasal delivery of nanoparticle encapsulated tarenflurbil: A potential brain targeting strategy for Alzheimer's disease. *Eur. J. Pharm. Sci.* **92**, 224–234 (2016).
80. Jafarih, O. *et al.* Design, characterization, and evaluation of intranasal delivery of ropinirole-loaded mucoadhesive nanoparticles for brain targeting. *Drug Dev. Ind. Pharm.* **41**, 1674–1681 (2015).
81. Joshi, A. S., Patel, H. S., Belgamwar, V. S., Agrawal, A. & Tekade, A. R. Solid lipid nanoparticles of ondansetron HCl for intranasal delivery: Development, optimization and evaluation. *J. Mater. Sci. Mater. Med.* **23**, 2163–2175 (2012).

Author contributions

S.A.S., K.Y.M., and N.A.E. conceptualized the project. All authors conducted the practical work of the project. K.Y.M. wrote the manuscript. S.A.S. revised the manuscript. S.A.S. supervised the project. K.Y.M. and N.A.E. assisted in supervising the project.

Funding

Open access funding provided by The Science, Technology & Innovation Funding Authority (STDF) in cooperation with The Egyptian Knowledge Bank (EKB).

Competing interests

The authors declare no competing interests.

Additional information

Correspondence and requests for materials should be addressed to S.A.S.

Reprints and permissions information is available at www.nature.com/reprints.

Publisher's note Springer Nature remains neutral with regard to jurisdictional claims in published maps and institutional affiliations.



Open Access This article is licensed under a Creative Commons Attribution 4.0 International License, which permits use, sharing, adaptation, distribution and reproduction in any medium or format, as long as you give appropriate credit to the original author(s) and the source, provide a link to the Creative Commons licence, and indicate if changes were made. The images or other third party material in this article are included in the article's Creative Commons licence, unless indicated otherwise in a credit line to the material. If material is not included in the article's Creative Commons licence and your intended use is not permitted by statutory regulation or exceeds the permitted use, you will need to obtain permission directly from the copyright holder. To view a copy of this licence, visit <http://creativecommons.org/licenses/by/4.0/>.

© The Author(s) 2023